Residual Stress and Thermal Expansion Coefficient of Plasma Polymerized Films

AKIRA MORINAKA and YOSHIHIRO ASANO, *Ibaraki Electrical Communication Laboratory, Nippon Telegraph and Telephone Public Corporation, Tokai, Ibaraki, 319-11, Japan*

Synopsis

The residual stress in plasma polymerized films and its annealing effect were measured by employing the Newton ring method. The plasma polymerized films studied were hexamethyldisiloxane (HMDS), norbornadiene (NBD), and acryronitrile (AN) films. The stress in the film is compressive, and this compressive stress changes into tensile stress by annealing treatment. The ESR measurement indicates that the annealing effect on the stress is due to the trapped radical reaction. From the thermal stress measurement, the thermal expansion coefficient and Young's modulus have also been obtained; Young's modulus is in the order of magnitude of 10^8 g/cm^2 with HMDS and NBD films, and the thermal expansion coefficient is in the order of magnitude of 10^{-5} deg^{-1} with HMDS and NBD films. These values are much different from those of conventional polymer. This is attributed to the highly crosslinked structure of the films.

INTRODUCTION

Highly crosslinked and pinhole-free films have been formed from many kinds of organic vapor by the use of plasma polymerization. The plasma polymerized films exhibit potentially useful properties such as dielectric films,[1] semipermeability membranes,[2,3] and photoconductive films.[4]

However, the plasma-polymerized film tends to crack and peel off from the substrate when its thickness grows to over several micrometers. These phenomena are due to the residual stress in the film. Therefore, it is important to know how the residual stress is caused and how to reduce the stress.

Yasuda et al.[5] reported the residual stress in plasma-polymerized film, estimated from the extent of curling of the low-density polyethylene substrate. They found that the residual stress is a compressive one, which is in a direction opposite to that in conventional polymer film. However, this stress depends on the polymerization mechanism, so that it would be sensitive to polymerization conditions. In addition, the highly crosslinked structure suggests that the physical properties of plasma polymerized film are also different from conventional polymer film properties.

This paper presents results of an investigation on the residual stress dependence in plasma-polymerized films on polymerization conditions. The stress in the film on a Si wafer was measured by the Newton ring method.[6–8] An attempt was made to relate the origin of the residual stress to the polymerization mechanism. The relationship between residual stress after annealing treatment and trapped radical relation is also discussed, based on the results of ESR measurement. Furthermore, the thermal expansion coefficient and Young's modulus for the plasma-polymerized film are obtained by employing the Newton ring method.

Journal of Applied Polymer Science, Vol. 27, 2139-2150 (1982)
© 1982 John Wiley & Sons, Inc.
CCC 0021-8995/82/062139-12$02.20

EXPERIMENTAL

Film Preparation

A diagram of the experimental apparatus for plasma-polymerized film deposition is shown in Figure 1. It essentially consisted of circular congruent parallel electrodes 70 mm in diameter positioned horizontally and separated by a 40-mm gap. The lower electrode was connected to the 13.56-MHz rf generator output through an impedance matching network. The substrate was placed on the upper electrode. Three kinds of monomer were used: hexamethyldisiloxane (HMDS), norbornadiene (NBD), and acryronitrile (AN), as typical monomers for siloxane, diene, and vinyl compounds, respectively. Monomer gas pressure was kept at 6.0×10^{-2} Torr during polymerization. The monomer gas flow rate was 4 STP cm^3/min, measured by a mass flow meter. Film thicknesses were measured by a surface tracer. Substrate thicknesses were measured by an electronic digital micrometer.

Stress Measurement

The stress in the film was measured by observing the radius of curvature of the substrate using the Newton ring method. For the stress measurement at elevated temperature, a cylindrical heating furnace, which enclosed a quartz optical flat, was used. The temperature of the sample was controlled and it can be heated to 200°C.

The stress σ_f in the film was calculated from the following equation[9]:

$$\sigma_f = \frac{E_s \cdot d_s{}^2}{6\,(1 - \nu_s)\,d_f}\left(\frac{1}{a_f} - \frac{1}{a_0}\right) \tag{1}$$

where a_0 and a_f are the radii of curvature for the substrate before and after the film deposition, E_s and α_s are Young's modulus and Poisson's ratio for the substrate, and d_s and d_f are the substrate and film thicknesses, respectively. The

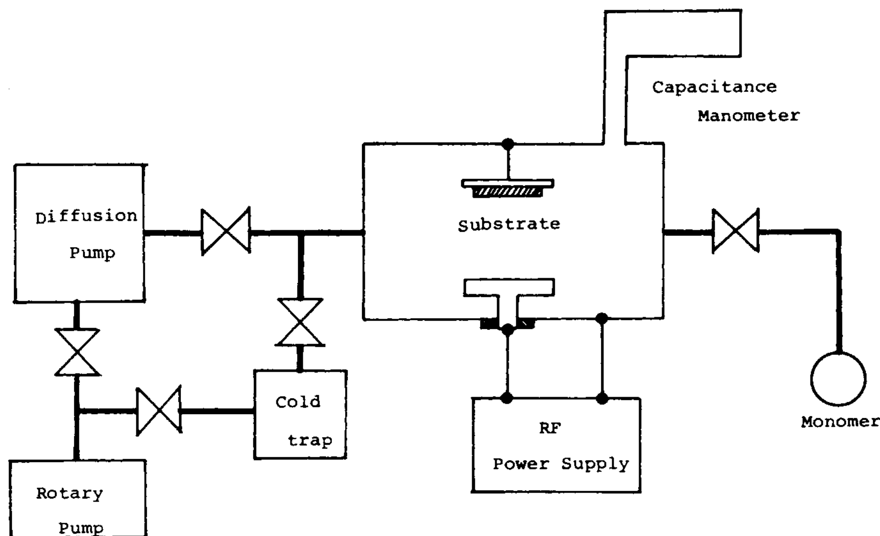

Fig. 1. Apparatus for manufacturing plasma-polymerized film.

substrates used were Si[(110)-oriented, 30 mm in diameter, 150 μm in thickness] and SiO_2 (fused quartz, 20 mm in diameter, 100 μm in thickness). For (110)-oriented Si substrate, $E_s/(1 - \nu_s) = 2.38 \times 10^9$ g/cm^2 and for SiO_2 substrate, $E_s/(1 - \nu_s) = 1.1 \times 10^9$ g/cm^2.[10,11]

Thermal stress σ_t, caused by the difference between the thermal expansion coefficients and for the film and the substrate, is expressed by[6]

$$\sigma_t = (\alpha_f - \alpha_s)\,[E_f/(1 - \nu_f)](T - T_d), \tag{2}$$

where α_f and α_s are the thermal expansion coefficients for film and substrate and E_f and α_f are Young's modulus and Poisson's ratio for the film, respectively. T is the temperature at which the stress is measured, and T_d the film deposition temperature.

ESR Measurement

The radical density of the film was measured by ESR. For ESR measurements, films were prepared on a glass substrate (100 μm in thickness). The signal strength generated from the glass, which was sputtered in Ar gas under the same rf power as polymerization, was smaller than 1% of it from the plasma-polymerized film. Therefore, the radical signal in the substrate was small enough to be neglected in our experiment.

The trapped radical signal shows Gaussian mode. Accordingly, signal strength S_G is given by[12]

$$S_G = \frac{1}{4}(\pi/2)^{1/2} \exp\left(\frac{1}{2}\right) \Delta H_{msl}{}^2\,(2h_0), \tag{3}$$

where ΔH_{msl} is the signal width and h_0 the signal height. S_G was calibrated by comparison with the signal from diphenyldipicrylhydrazyl (DPPH) standard solution of known spin density.

RESULTS

Deposition Rate

Figure 2 shows the film thicknesses as a function of polymerization duration for HMDS, NBD, and AN films at various rf powers. Film thickness increases linearly with polymerization duration. This means that the polymerization condition is retained constant during film deposition. The deposition rate increases with an increase of rf power and decreases with a rise of the substrate temperature. These results suggest that the deposition rates depend on the quantities of adsorbed monomers on the substrate and reactive species in vapor phase.[13]

IR Spectra

The plasma-polymerized film is considerably different in structure from the film prepared by the conventional polymerization method. IR spectra were measured in order to investigate the structures of the plasma polymerized films at various rf powers. In Figures 3, 4, and 5, IR spectra for HMDS, NBD, and AN films are shown in comparison with those for individual monomers.

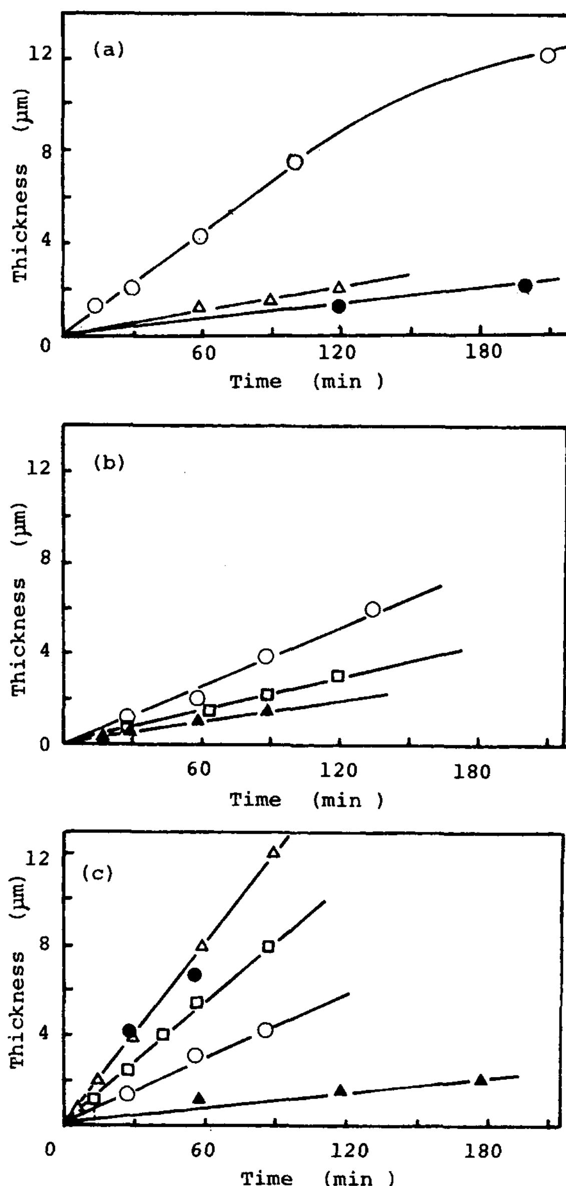

Fig. 2. Relation between film thickness and polymerization polymerization. (a) HMDS films [(○) 40 W, room temperature (RT); (△) 4 W, RT; (●) 40 W, 300°C]; (b) AN films [(○) 40 W, RT; (□) 20 W, RT; (▲) 4 W, RT]; (c) NBD films [(●) 40 W, RT; (△) 20 W, RT; (□) 10 W, RT; (○) 5 W, RT; (▲) 20 W, 300°C]. Polymerization conditions: 6.0×10^{-2} Torr, 4 STP cm^3/min, 13.56 MHz.

The spectra of HMDS films show a decrease in S_i—CH_3 absorption at 2980 cm^{-1} and 1250 cm^{-1} with the increase of rf power. On the other hand, S_i—O absorption at 1050 cm^{-1} does not show an appreciable change with the increase of rf power. In the spectra of NBD films, a bicyclo-bridged methylene absorption at 1300 cm^{-1} disappears, and additional peaks, which may be attributed to *trans*-vinyl absorption appear, at 1680 cm^{-1} and 980 cm^{-1}. In the spectra of

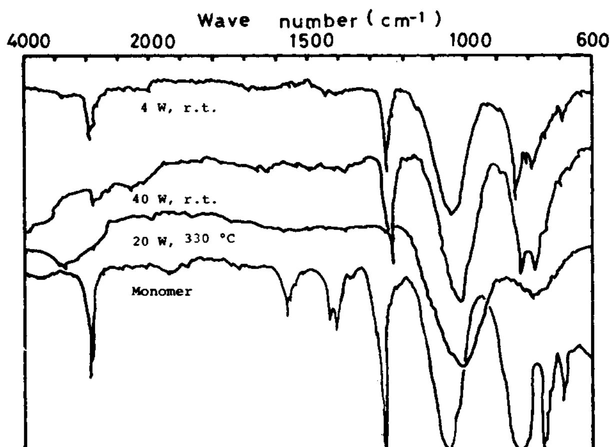

Fig. 3. IR spectra for HMDS films at various rf powers.

AN films, a nitrile absorption at 2250 cm^{-1} decreases with the increase of rf power and additional peaks assignable to Shiff's base (—CH=NH and —CH=N—) appear at 3500 cm^{-1} and 1500 cm^{-1}. From these results, it can be seen that, at low rf power, the monomer structures remain in the films, and, at high rf power, crosslinked structures are formed in the films by the scission of main chain or side groups.

Residual Stress in Films

Figure 6 shows the residual stress for HMDS, NBD, and AN films deposited at room temperature as a function of rf power. All films were subjected to compressive stress, and the samples became concave as viewed from the substrate side. The stress in the HMDS film is 5×10^4 g/cm^2 at 40-W rf power, in the NBD film it is 1.2×10^5 g/cm^2 at 20-W rf power, and in the AN film it is 4.9×10^5 g/cm^2 at 20-W rf power, respectively. The stress in the HMDS film is as small as $1/10$ of those of other films. The stress in the hexamethyldisilazane film was also in the order of 10^4 g/cm^2.

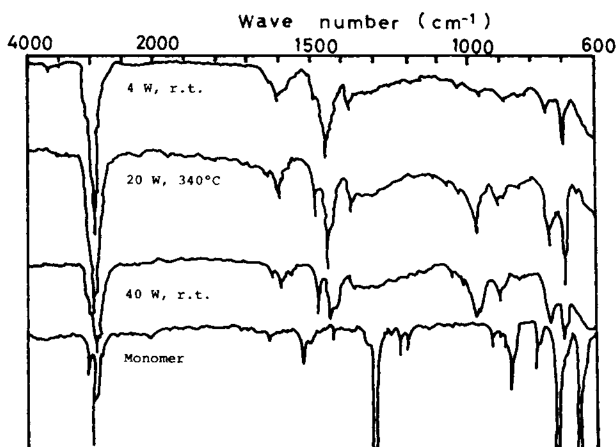

Fig. 4. IR spectra for NBD films at various rf powers.

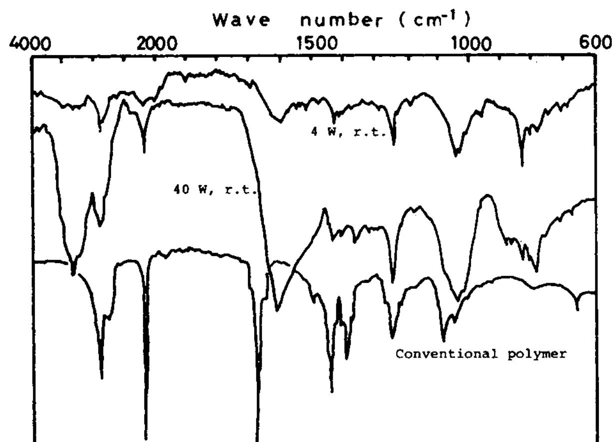

Fig. 5. IR spectra for AN films at various rf powers.

The stresses in all films are independent of film thicknesses. This means that the cracking of film does not occur at a relatively great thickness and the polymerization condition is retained as constant during the film deposition. On the other hand, the stress increases with the increase of rf power. Comparing with the results of IR spectra, it is seen that the stress increases with increasing of the crosslinked structure.

The stress in the HMDS film deposited at elevated temperature is shown in Figure 7 vs. the deposition temperature. The stress is tensile and increases with the rise of deposition temperature. This tensile stress is attributed to the thermal stress caused by the difference between the thermal expansion coefficients of the film and the substrate.

Annealing Effect on Stress and Trapped Radical Density

Stresses in HMDS and NBD films are plotted against annealing temperature in Figures 8 and 9. The values of the stress were measured at room temperature after annealing in vacuum for 120 min. In AN films, cracking of the film occurred due to annealing treatment, so that the annealing effect on stress could not be

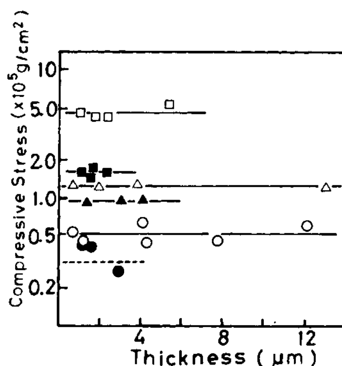

Fig. 6. Residual stresses in plasma-polymerized films deposited at room temperature vs. film thickness. AN film: 20 W (□); 5 W (■); NBD film: 20 W (△); 5 W (▲). HMDS film: 40 W (○); 4 W (●).

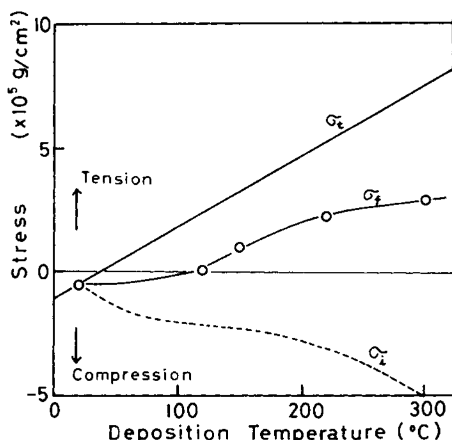

Fig. 7. Residual stress (σ_f), thermal stress (σ_T), and intrinsic stress (σ_i) in the HMDS film deposited at elevated temperature vs. film deposition temperature. Polymerization conditions: 6.0 $\times$ 10^{-2} Torr, STP cm^3/min, 40-W rf power.

observed. After annealing treatment, the HMDS and NBD films were subjected to tensile stress; i.e., the direction of the stress changes from compression to tension by annealing. Once the films were annealed, the stress did not change any more below annealing temperature.

In order to investigate the relation between the annealing effect on stress and the trapped radical, radical density is measured. The radical density in the films were measured by ESR. Results are summarized in Table I. In the as-deposited samples, the radical density corresponds to the magnitude of stress; i.e., the radical density as well as the stress becomes smaller in the order of AN, NBD, and HMDS films, and increases with an increase of rf power. The radical density in HMDS and NBD films decreases due to the annealing at 300°C for 120 min in vacuum. On the other hand, the AN film shows an increase of radical density caused by the annealing temperature. In general, heat treatment is considered to produce both the trapped radical reaction and the decomposition in the plasma

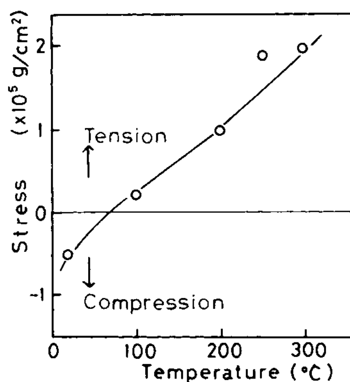

Fig. 8. Annealing effect on stress in the HMDS film deposited at room temperature. Polymerization conditions: 6.0 $\times$ 10^{-2} Torr, 20-W rf power. Annealing conditions: 300°C, 100 min.

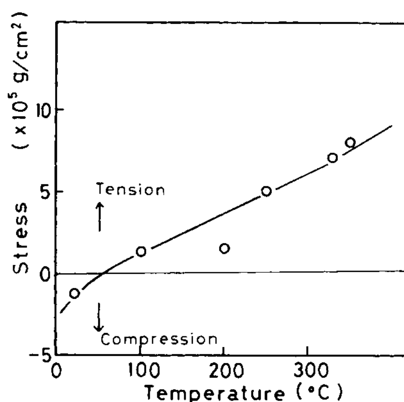

Fig. 9. Annealing effect on stress in the NBD film deposited at room temperature. Polymerization conditions: 6.0×10^{-2} Torr, 20-W rf power. Annealing conditions: 300°C, 100 min.

polymerized film.[14] In the annealing temperature range pertinent to this study, the radical reaction seems to prevail against the decomposition in HMDS and NBD films. Conversely, in the AN film, the decomposition is considered to prevail against the radical reaction.

In Figure 10, the radical density as well as the stress in the HMDS film annealed at various temperatures up to 200°C are shown vs. the annealing time. Radical density was measured at room temperature after annealing, and the stress was measured at the annealing temperature. Radical density in the HMDS film decreases with annealing time up to 60 min and tends to a constant value at annealing time beyond 60 min. As can be seen in Figure 10, the annealing characteristics of stress show the same tendency as the change of radical density; i.e., the tensile stress of the film increases with the annealing time and tends to a constant value at annealing time beyond 60 min. These results suggest that the tensile stress is caused by the trapped radical reaction.

Young's Modulus and Thermal Expansion Coefficient

Figures 11 and 12 show the temperature dependence of curvature of HMDS and NBD films deposited at 40-W rf power on Si and SiO_2 substrates. The HMDS films were annealed at 300°C for 120 min in vacuum. As described in the previous subsections, once the film was annealed, the stress did not change any more. Therefore, the temperature dependence of curvature is attributed

TABLE I
Radical Density in Plasma-Polymerized Film

Monomer	rf power (W)	Radical density (spins/g) As deposited	Radical density (spins/g) After annealing[a]
HMDS	10	7.0×10^{17}	5.3×10^{17}
	40	1.4×10^{18}	5.2×10^{17}
NBD	4	6.0×10^{17}	2.3×10^{17}
	20	8.5×10^{18}	3.2×10^{18}
AN	4	4.4×10^{18}	1.0×10^{20}
	20	9.8×10^{18}	1.0×10^{20}

[a] Annealing condition: 300°C for 120 min in vacuum.

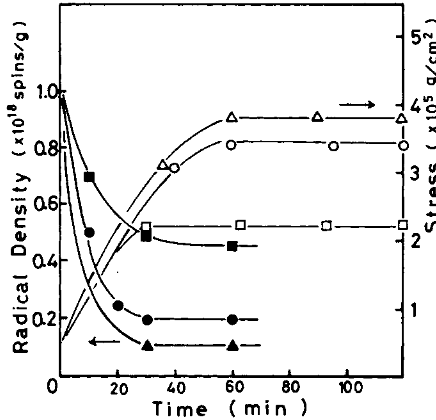

Fig. 10. Variation of stress and radical density in the HMDS film vs. annealing time. Stress was measured at elevated temperature: 50°C (■); 100°C (●); 150°C (▲). Radical density was measured at room temperature after annealing treatment. Annealing temperatures were: 100°C (□); 150°C (○); 200°C (△).

to the thermal stress. From eqs. (1) and (2),

$$\left(\frac{1}{a_f} - \frac{1}{a_0}\right) = \frac{6E_f \cdot d_f}{E_s \cdot ds^2} \frac{(1 - \nu_s)}{(1 - \nu_f)} (\alpha_s - \alpha_f)(T - T_d) \qquad (3)$$

As shown in Figure 11, $1/a_f$ decreases linearly with the increase of T. This means that α_f, E_f, ν_f, ν_s, E_s, and α_s are independent of the temperature in the temperature range pertinent to this study. Accordingly, from the difference in the gradients for the two lines in Figure 11, α_f and E_f for the HMDS film are estimated to be 1.4×10^4 g/cm^2 and 1.8×10^{-5} deg^{-1}, respectively. In this estimation, the value of ν_f was assumed to be 0.3. In Figure 12, the curvature values for NBD films deposited at 20-W rf power on Si and SiO_2 substrates are shown as a function of the measuring temperature. The NBD films were annealed at 250°C for 120 min in vacuum. In the same way as the HMDS film, the values of α_f and E_f for the NBD film are estimated to be 1.4×10^{-5} deg^{-1} and 1.8×10^5 g/cm^2, respectively. The values for α_f and E_f may depend on the polymerization condition. It is clear, however, that the HMDS and NBD films have much smaller α and larger E than conventional polymer film. For example, α and E for polyethylene are $6 \sim 8 \times 10^{-5}$ deg^{-1} and $0.2 \sim 0.02 \times 10^8$ g/cm^2, respectively.

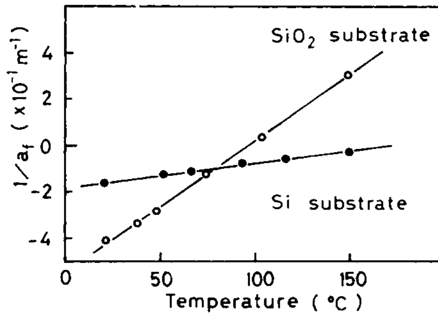

Fig. 11. Temperature dependence of curvature for Si and SiO_2 substrates with the HMDS films after annealing. Polymerization conditions: 6.0×10^{-2} Torr, 20-W rf power, RT.

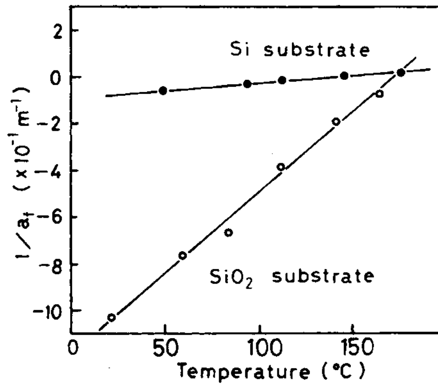

Fig. 12. Temperature dependence of curvature for Si and SiO_2 substrates with the NBD films after annealing. Polymerization conditions: 6.0×10^{-2} Torr, 20-W rf power, RT.

DISCUSSION

When the film is deposited at room temperature, the stress σ_f in the film at room temperature is only the intrinsic stress σ_i produced during polymerization. The origin of σ_i has been reported as follows[5]: Monomers are activated in gas phase by electron bombardment and then diffuse to the substrate. These monomers react with the already laid down polymerized film and wedge between existing polymer chain segments. This wedging gives the compressive stress σ_i in the film.

The experimental results obtained in this study support this explanation. The concentration of reactive monomer in gas phase increases as rf power increases. Accordingly, it is expected that the film deposition rate, the degree of cross-linking, the trapped radical density, and σ_i will increse together with the increase of rf power.

When the film is deposited at elevated temperature, the stress σ_f is considered to be the sum of σ_i and the thermal stress σ_t. σ_i is compressive and σ_t is tensile, from the fact that $\alpha_s < \alpha_f$. Accordingly, σ_f is given by

$$\sigma_f = \sigma_i - \sigma_t. \tag{4}$$

In the case of the HMDS film deposited on Si substrate, by substituting E_f and α_f obtained in the last subsection of the previous section into eq. (2), we have

$$\sigma_t = 2.88 \times 10^3 (T - T_d). \tag{5}$$

In Figure 7, σ_f, σ_t, and σ_i for the HMDS film deposited on Si substrates are shown as a function of the deposition temperature. σ_i increase with the rise of deposition temperature. This is explained as follows. The concentration of reactive monomers in the gas phase is independent of the deposition temperature. On the other hand, the film deposition rate decreases with the rise of deposition temperature. Therefore, a higher deposition temperature generates a higher degree of wedging per unit volume in the resultant film.

The annealing effect on the stress is considered to be related to the trapped radical reaction in the film. At elevated temperature, the sample became convex due to the thermal stress. Radicals react with each other under such a situation, so that the tensile stress remains in the film even after return to room tempera-

ture. Consequently, the compressive stress produced during polymerization can be reduced by annealing treatment at an optimum temperature.

One feature of the plasma polymerized film is the high degree of crosslinking. This is the reason why the thermal expansion coefficients and Young's moduli for the HMDS and NBD films are different from those of conventional polymer, such as polyethylene. Therefore, it would be expected that the thermal expansion coefficient and Young's modulus for the plasma-polymerized film with a high degree of crosslinking are in the same order of magnitude as those for HMDS film.

SUMMARY

The results obtained are summarized as follows:

(1) The HMDS, NBD, and AN films deposited at room temperature were subjected to compressive stress. The stresses in HMDS, NBD, and AN films were 5×10^4 g/cm^2, 1.3×10^5 g/cm^2, and 4.9×10^5 g/cm^2, respectively. The compressive stress increased with the increase of rf power.

(2) The stresses in HMDS and NBD films, deposited at elevated temperature above 100°C, was tensile. This tensile stress was attributed to the thermal stress and increased with the rise of deposition temperature. Furthermore, the compressive stress produced during polymerization increased with the rise of deposition temperature.

(3) The compressive stress in HMDS and NBD films changed into tensile stress by annealing treatment. This annealing effect on the stress was considered to be related to the trapped radical reaction in the film from the ESR measurement. The annealing treatment at an optimum temperature makes it possible to reduce the stress in the film.

(4) From the thermal stress measurement, the thermal expansion coefficient α and Young's modulus E have been obtained; for the HMDS film, α and E were 1.8×10^{-5} deg^{-1} and 1.4×10^8 g/cm^2, and for the NBD film α and E were 1.4×10^{-5} deg^{-1} and 1.8×10^8 g/cm^2, respectively.

The authors would like to acknowledge the continuing guidance and encouragement from Drs. K. Matsuyama and H. Yaginuma.

References

1. A. M. Mearns, *Thin Solid Film*, **3,** 201 (1969).
2. K. B. Buck and V. K. Dava, *Br. Polym. Sci.*, **2,** 238 (1970).
3. H. Yasuda and C. E. Lamaze, *J. Appl. Polym. Sci.*, **15,** 2227 (1971).
4. A. Bradley and J. P. Hammes, *J. Electrochem. Soc.*, **110,** 15 (1969).
5. H. Yasuda, T. Hirotsu, and H. G. Olf, *J. Appl. Polym. Sci.*, **21,** 3179 (1977).
6. J. A. Aboaf, *J. Electrochem. Soc.*, **12,** 1732 (1969).
7. H. Sunami, Y. Itoh, and K. Sato, *J. Appl. Phys.*, **41,** 5115 (1970).
8. M. Tamura and H. Sunami, *Jpn. J. Appl. Phys.*, **11,** 1097 (1973).
9. R. J. Jaccodine and W. A. Schlegel, *J. Appl. Phys.*, **37,** 2429 (1966).
10. J. J. Wartman and R. A. Evans, *J. Appl. Phys.*, **36,** 153 (1965).

11. Chemical Rubber Co., *Handbook of Chemistry and Physics*, CRC Press, Cleveland, 1968.
12. R. S. Alger, *Electron Paramagnetic Resonance*, Interscience, New York, 1968.
13. D. K. Lam and R. F. Baddour, *J. Macromol. Sci.*, **A10,** 501 (1976).
14. S. Morita, G. Sawa, and M. Ieda, *J. Macromol. Sci.*, **A10,** 421 (1976).

Received December 18, 1980
Accepted December 21, 1981